

# Coordinated Chemomechanical Cycles: A Mechanism for Autonomous Molecular Motion

S. J. Green, J. Bath, and A. J. Turberfield\*

*University of Oxford, Department of Physics, Parks Road, Oxford OX1 3PU, United Kingdom*

(Received 15 February 2008; revised manuscript received 10 September 2008; published 3 December 2008)

The second law of thermodynamics requires that directed motion be accompanied by dissipation of energy. Here we demonstrate the working principles of a bipedal molecular motor. The motor is constructed from DNA and is driven by the hybridization of a DNA fuel. We show how the catalytic activities of the feet can be coordinated to create a Brownian ratchet that is in principle capable of directional and processive movement along a track. This system can be driven away from equilibrium, demonstrating the potential of the motor to do work.

DOI: 10.1103/PhysRevLett.101.238101

PACS numbers: 87.15.hj, 81.07.Nb, 81.16.Dn, 87.14.gk

Unidirectional motion in a dissipative environment requires expenditure of free energy: to create a molecular motor that is capable of transducing energy is a formidable experimental challenge. A light-driven molecule that rotates continuously and unidirectionally about a covalent bond [1] was a breakthrough in artificial molecular machinery. Most chemically fueled synthetic molecular machines, however, are not autonomous: they require a sequence of control signals, each of which switches the motor to a new stable configuration. These transitions involve control of charge states [2] or making and breaking covalent [3,4] or noncovalent bonds [5–9]. Synthetic machines made from DNA [10], including walkers [7,8] and molecular rotors [9], use energy provided by DNA base-pairing to generate motion: they are operated by addition of control strands of DNA, and duplexes formed by hybridization of control strands are produced as waste products. Limited autonomous linear motion has been achieved by a device that uses natural enzymes to couple hydrolysis of adenosine triphosphate (ATP) to a cycle of DNA cleavage and ligation [11]. Linear motion has also been achieved by DNA devices that irreversibly create or damage a track [12–15].

An autonomous molecular motor that does not alter its track needs an external energy source: if it uses a chemical fuel, it must be a catalyst that couples chemical change to mechanical motion. Here we demonstrate the mechanism of a chemically fueled motor that is designed to transport a load on a reusable track and to operate without intervention until it runs out of fuel. The motor is built from DNA, and the free energy required for directional motion is obtained by catalyzing hybridization of a DNA fuel [5,6]. Its two-footed structure is inspired by kinesin [16] and myosin V [17], protein motors with two feet (or “heads”) that are driven along cytoskeletal filaments by ATP hydrolysis. The DNA motor’s feet are coordinated by means of competition where their binding sites on the track overlap: competition exposes different ends of the identical feet so that the left and right feet interact with the fuel at different rates. We show how the catalytic activities of the two feet can be

coordinated to create a Brownian ratchet [18,19] that is in principle capable of directional and processive movement.

Each cycle of operation is tightly coupled to the reaction of one fuel molecule (Fig. 1). In state 0 the feet are bound to adjacent sites on the periodic track. A fuel molecule can bind to either foot, displacing it from the track ( $0 \rightarrow 1$ ). The lifted foot catalyzes decomposition and dissociation of the fuel ( $1 \rightarrow 2$ ) and can then rebind the track on either side of the stationary foot ( $2 \rightarrow 0$ ). Each transition is driven by a significant decrease in free energy ( $|\Delta G| \gg k_B T$ ). The track is directional, allowing discrimination between feet according to their relative positions. All positions of the motor in state 0 have the same energy. In equilibrium, a bias to picking up the left foot  $\alpha = k_{01L}/k_{01R}$  would be exactly cancelled by a bias favoring replacement of a lifted foot to the left  $\beta = k_{20L}/k_{20R}$  such that  $\alpha/\beta = 1$ : there would be no directional motion. However, dissipation of free energy in a nonequilibrium transition  $1 \rightarrow 2$  uncouples detachment and reattachment processes. We have achieved a bias towards picking up the left foot ( $\alpha \gg 1$ ) without reattachment bias ( $\beta \approx 1$ ). This combination, indicated by bold arrows, is sufficient to create directional motion.

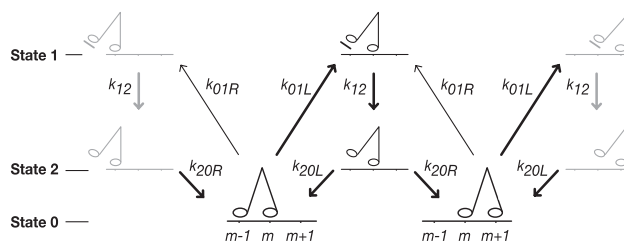


FIG. 1. Kinetic scheme. Identical feet bind adjacent sites on the track (state 0). Fuel can bind to either foot, displacing it from the track (state 1). The lifted foot catalyzes reaction of the fuel, freeing the foot (state 2) and allowing it to be replaced. Engineered bias towards lifting the left foot, with unbiased reattachment, drives the motor to the right (bold arrows). Effective first order rate constants are labeled according to the position (left or right) from which the foot is lifted ( $k_{01L}$ ,  $k_{01R}$ ) or to which it is replaced ( $k_{20L}$ ,  $k_{20R}$ ).

The motor (Fig. 2 and Table I) is powered by DNA hybridization, i.e., formation of a Watson-Crick double helix between complementary strands of DNA. The fuel consists of two DNA hairpin loops with complementary 18-nucleotide (nt) loop domains  $L$  or  $\bar{L}$  held closed by hybridization of 9-nt neck domains  $N$  and  $\bar{N}$ . Hairpin  $H1$  ( $\bar{N}LNT$ ) is complementary to hairpin  $H2$  ( $\bar{N}\bar{L}N$ ), except that  $H1$  also has a 6-nt toehold domain [20]  $T$  at the 3' end (domain sequences are written 5'  $\rightarrow$  3'). For hairpin concentrations of  $10^{-6}$  M and a waste-product concentration  $[H1 \cdot H2] = 10^{-6} \sim 10^{-9}$  M,  $\Delta G_{\text{hyb}} = -30 \sim -34 \text{ kcal mol}^{-1}$  ( $50 \sim 60 k_B T$ ) [21], comparable to the free energy of hydrolysis of ATP at typical cellular concentrations ( $\Delta G_{\text{ATP}} = -12 \text{ kcal mol}^{-1}$ ,  $20 k_B T$ ). (See sup-

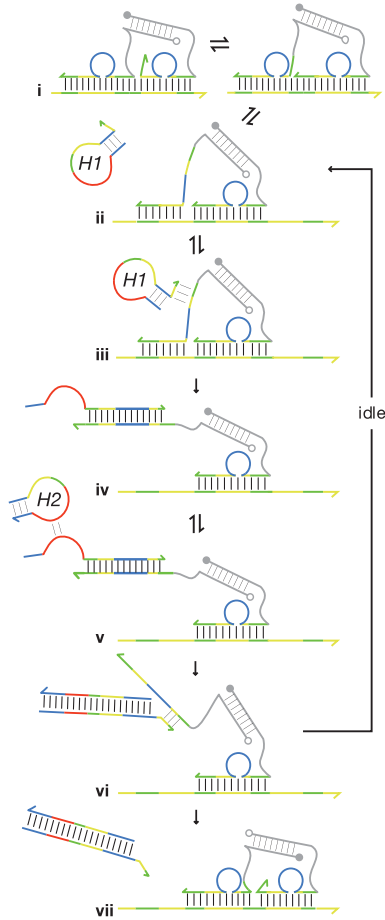


FIG. 2 (color). Motor design. The two-part fuel consists of complementary hairpins  $H1$  and  $H2$ . Competition between feet for binding to the track (i) can lift part of the left foot from the track to reveal a toehold domain (ii). This can bind the complementary toehold domain of  $H1$  (iii), initiating a strand-displacement reaction that opens the neck of  $H1$  and displaces the left foot from the track (iv). Part of the opened loop  $H1$  can act as a second toehold to initiate hybridization with  $H2$  (v) to form a stable waste product (the  $H1 \cdot H2$  duplex), displacing  $H1$  from all but the initial toehold domain of the lifted foot (vi) and allowing the foot to rebind the track to the left or right with equal probability (vii).

plementary material [22] Fig. S1 for an investigation of interactions between  $H1$  and  $H2$  [23–25].) Both components of the fuel are added simultaneously, but spontaneous hybridization of  $H1$  and  $H2$  is inhibited by the closure of their necks. Reaction of the fuel can be catalyzed by the formation of a transient complex in which the neck of  $H1$  is opened by a catalytic sequence  $\bar{T}\bar{N}$  [6,10,14,23–25]. This catalyst is incorporated in the feet of the motor. The feet are identical but, as described below, the catalytic activity of the foot in the left position is much greater than that of the right foot. Each motor step is coupled to catalysis of one  $H1 - H2$  hybridization reaction. Hairpin  $H1$  binds preferentially to the left foot, lifting the foot from the track and opening the loop;  $H1$  then reacts with  $H2$ , allowing the foot to be replaced on the track to the left or the right with equal probability.

The motor's single-stranded feet are attached via 4-nt linkers to an 18-base pair (bp) double-stranded spacer. The track is also single-stranded DNA (its 5' end is drawn on the left). The track consists of alternating binding and competition domains  $B$  and  $C$  (12 and 6 nt, respectively). Each foot includes the domain sequence  $\bar{C}\bar{B}_1\bar{N}\bar{B}_2\bar{C}$  ( $\bar{B}_1\bar{B}_2 \equiv \bar{B}$ ): Figure 2 shows in (i) how the feet hybridize to track domains  $CBC$ , pinching off domain  $\bar{N}$  as a bulge loop. The feet are constrained by the length of the spacer to bind to overlapping sites where they compete for binding to a central domain  $C$ : this is the basis for discrimination between feet.

$\bar{B}_1$  and the two nucleotides at the 3' end of the adjacent  $\bar{C}$  form a toehold domain  $\bar{T}$ . The catalytic activity of the left foot is activated when its toehold domain is exposed by competition from the right foot (ii) ( $\bar{C}$  is displaced by direct

TABLE I. Nucleotide sequences written 5'  $\rightarrow$  3'. Functional domains  $B$ ,  $C$ ,  $\bar{B}$ ,  $\bar{C}$ , etc., are indicated by color. Single-stranded spacer domains are in lower case.

Strands	
$H1^a$	ATCTTGATGATGAGGTGAACGAGCAGCATCAAGATGTCAAC
$H2$	ATCTTGATGCTGCTCGTTCACCTCATCAAGAT
$f1$	GTGCGATTCCCTCAATAC(t) <sub>4</sub> TTCAGTTGACATCTTGATGCTGCTCGTTCAGT
$f2$	GTATTGAGGGAATCGCAC(t) <sub>4</sub> TTCAGTTGACATCTTGATGCTGCTCGTTCAGT
$f3$	GTATTGAGGGAATCGCAC(t) <sub>4</sub> TTCAGTAAGTATCGGATCTTTCAGT
$f4^b$	GTATTGAGGGAATCGCAC(t) <sub>4</sub> TTCAGTAAGT(t) <sub>10</sub> ATCGGATCTTTCAGT
$t$	(t) <sub>10</sub> ACTGAAAGAGCAGCGTCAACTGAAAGAGCAGCGTCAACTGAA(t) <sub>10</sub>
$t_L$	ACTGAAAGAGCAGCGTCAACTGAAAGATCCGATACTTACTGAA
$t_R$	ACTGAAAGATCCGATACTTACTGAAAGAGCAGCGTCAACTGAA
$t_C^c$	GATACTTACTGAAAGAGCAGCGTCAACTGAAAGAGCAGCGTCAACTGAAAGATCC
Domains	
$B$	CGAGCAGCGTCA
$C$	ACTGAA
$L$	ATGAGGTGAACGAGCAGC
$N$	CATCAAGAT
$T1$	ATGAGG
$T$	GTCAAC

<sup>a</sup>3' carboxytetramethylrhodamine (TAMRA) [Fig. 3(b) only].

<sup>b</sup>5' tetrachlorofluorescein (TET).

<sup>c</sup>5' phosphate.

competition and the short (4 nt)  $\bar{B}_1$  dissociates spontaneously).  $\bar{T}$  can hybridize to toehold  $T$  on  $H1$  (iii) to initiate a strand-displacement reaction in which domain  $\bar{N}$  of the left foot displaces the equivalent domain in the hairpin's neck to open the loop [6,14,24,25]. Part of loop domain  $L$  can then displace the rest of the foot from the track (iv). An unprotected toehold can accelerate a strand-displacement reaction by up to 7 orders of magnitude [20]. The identical right foot is unreactive because its toehold suffers no competition and remains hybridized to the track. There is thus a designed kinetic bias to picking up the left foot ( $\alpha > 1$ ).

When a foot is raised from the track, six unhybridized nucleotides at the 5' end of opened loop domain  $L$  can act as an internal toehold ( $TI$ ) [6,10,23,24] to initiate reaction between  $H1$  and  $H2$  (v) to form the stable waste product  $H1 \cdot H2$  (vi), freeing the raised foot to rebind the track (vii) with no designed discrimination between sites to the left and right of the stationary foot ( $\beta \approx 1$ ). The toehold on the stationary foot remains hybridized to the track, so the probability that the motor will be displaced before the raised foot rebinds is low.

Figure 3(a) shows polyacrylamide gel electrophoresis (PAGE) analysis of the motor on a two-site track. The gel-purified motor migrates as a single band (lane 1). When  $H1$  is added at 23 °C (lane 2) only the band corresponding to a lifted left foot appears, consistent with the designed lifting bias. (Slow rearrangement of feet on the track removes this bias after 30 min, see supplementary material: Fig. S2 [22].) Only when the motor is annealed with  $H1$  (lane 3) are both feet lifted.

The kinetics of foot-fuel interactions are measured using a heterodimeric motor with one wild-type (normal) foot and one mutated foot which carries wild-type competition

domains  $\bar{C}$  but mutated domains  $\bar{B}_1\bar{N}\bar{B}_2$ : the mutated track-binding domain  $\bar{B}$  can be fixed in a known position on a modified track. Fluorophores are conjugated to the wild-type foot (TET donor) and fuel  $H1$  (TAMRA acceptor): TET fluorescence is quenched by Förster resonance energy transfer (FRET) on fuel binding and recovers when the fuel is displaced (see supplementary material Fig. S3 [22]). Figure 3(b) shows analysis of foot-fuel interactions on two-site tracks which position the wild-type foot to the left or to the right.  $H1$  binds rapidly to a wild-type left foot ( $k_{01L} = 5.8 \times 10^4 \text{ M}^{-1} \text{ s}^{-1}$ ). Binding to a wild-type right foot is 2 orders of magnitude slower ( $\alpha \approx 100$ ), as designed. The fitted second-order rate constant for replacement of the foot on the track on addition of  $H2$  is  $9.6 \times 10^3 \text{ M}^{-1} \text{ s}^{-1}$  with no significant bias to left or right ( $\beta \approx 1$ ). Measurement of the kinetics of foot-fuel interaction for a motor with two wild-type feet confirms that the bound foot is unreactive until displaced by heating: the probability that it will be lifted by  $H1$  before the raised foot rebinds in the presence of  $H2$  is approximately  $10^{-3}$  (see supplementary material: Fig. S5 [22]). These experiments confirm that the mechanism has the characteristics required for directionality ( $\alpha/\beta \neq 1$ ) and processivity (the probability that both feet will be displaced is low).

The capacity of the hybridization motor to do work is demonstrated by PAGE analysis of a heterodimeric motor on a three-site circular track to which the fixed foot is bound between two wild-type sites [Fig. 3(c)]. The circular track has no unhybridized competition domains  $C$  when both feet are bound, inhibiting the slow rearrangement of feet between sites that results from the flexibility of the test tracks (see supplementary material Fig. S2 [22]). Bands corresponding to both positions of the wild-type foot are seen (lane 1): asymmetry between the feet (the fixed foot

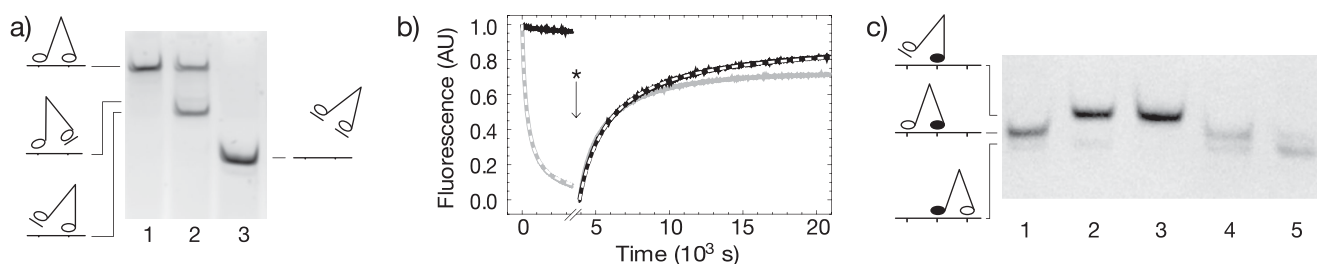


FIG. 3. Directionality and capacity to do work. (a) PAGE analysis of motor  $f1 \cdot f2$  on two-site track  $t$  showing discrimination between feet (see supplementary material Fig. S2 for band assignments [22]). 40 nM gel-purified track-bound motor (lane 1) was incubated with fuel  $H1$  (200 nM) for 2 min at 23 °C (lane 2) or annealed with  $H1$  by heating to 96 °C and cooling to 23 °C over 20 min (lane 3). (b) FRET measurements of foot-fuel interaction rates using tracks  $t_L, t_R$  that position the wild-type foot of heterodimeric motor  $f1 \cdot f4$  to the left (gray) or right (black) of its fixed foot ( $[f1 \cdot f4 \cdot t_{L,R}] = [H1] = 50 \text{ nM}$ ). At \* the reaction mixture was annealed, by heating to 85 °C for 10 min and cooling to 21 °C over 180 min to melt and reform in approximately equilibrium configuration all hybridization bonds, ensuring that all wild-type feet were lifted; fuel  $H2$  (50 nM) was then added. Dashed curves are fits to second-order kinetics (see text). (c) PAGE analysis of gel-purified heterodimeric motor  $f1 \cdot f3$  bound to circular track  $t_C$  showing that fuel can drive the motor out of equilibrium (supplementary material Fig. S4 shows full gel [22]). Lane 1: Motor + track ( $[f1 \cdot f3 \cdot t_C] = 100 \text{ nM}$ ). The wild-type foot can bind on either side of the fixed foot (colored black) giving bands with different mobilities. Track-bound motor was incubated with fuel  $H1$  (100 nM) for 90 min at 23 °C (lane 2) or annealed with  $H1$  by heating to 96 °C and cooling to 23 °C over 20 min (lane 3). Lane 4: Annealed sample after incubation with complementary fuel  $H2$  (100 nM). Lane 5: Track-bound motor incubated with excess of  $H1$  (200 nM) and  $H2$  (250 nM).

has no loop) biases the equilibrium such that most wild-type feet bind on the left (band assignments are discussed in the supplementary material Section 4). When incubated with fuel *H1* (lane 2), only wild-type left feet react readily. When the reaction is annealed (lane 3) wild-type feet in *both* positions are lifted. On subsequent addition of complementary fuel *H2* to the annealed sample (lane 4) all feet are replaced, with a near-equilibrium distribution between left and right sites. On incubation with both *H1* and *H2* (lane 4) the intensities of the bands are switched: the motor has been driven to the right hand position, out of equilibrium, using chemical energy from its fuel.

To analyze the expected performance of the motor on an extended track we solve the system of first order rate equations defined by Fig. 1 for the probabilities of occupancy of states 0, 1 and 2 in the steady state. (Foot lifting and replacement may be treated as first order reactions if the fuel concentrations are constant.) A load  $f$ , applied to the central spacer, which opposes the designed motion from left to right is modeled by favoring foot replacement in the left position by a factor  $\exp(f d / k_B T)$  where  $d$  is the distance between transition states for forward and backward steps. The average forward velocity (from left to right) is then

$$v = k_{\text{eff}} d \left( \frac{1}{1 + \alpha^{-1}} - \frac{1}{1 + \beta^{-1} e^{-f d / k_B T}} \right), \quad (1)$$

where

$$k_{\text{eff}}^{-1} = (k_{01L} + k_{01R})^{-1} + k_{12}^{-1} + (k_{20L} e^{f d / 2 k_B T} + k_{20R} e^{-f d / 2 k_B T})^{-1}. \quad (2)$$

The effective rate constant is limited by foot replacement:  $k_{\text{eff}} \sim 10^4 \text{ M}^{-1} \text{ s}^{-1} \times [H2]$ ,  $\alpha \approx 100$  and  $\beta \approx 1$ . We take  $d$  to be the distance between binding sites:  $d \approx 6 \text{ nm}$ . The stall force can be estimated by setting  $v = 0$ :

$$f_{\text{stall}} = \frac{k_B T}{d} \ln \frac{\alpha}{\beta} \approx 3 \text{ pN}. \quad (3)$$

This is comparable to forces exerted by myosin V [17] and kinesin [16].

Our motor is a Brownian ratchet [18,19]: movement of the lifted foot is driven solely by thermal fluctuations, and the fuel is used to provide the energy necessary to rectify this motion by breaking the detailed balance between lifting and replacing the front and back feet. Mechanistic models of myosin V and kinesin also incorporate diffusional searches, but these are biased to a forward binding site by the conformations of the bound foot and linker [26,27]. An optimized design would use reaction of the fuel to drive motion directly in a power stroke [19]. Coordination of the chemomechanical cycles of the two feet is essential to the directional and processive operation of these motors. Our designed cycle of fuel-induced unbinding, catalysis and rebinding is similar to the actomyosin cycle [28], and the mechanism that coordinates the

mechanochemistry of the feet is analogous to the strain-dependent nucleotide exchange mechanism that makes release of the back foot of myosin V dependent on binding of the front foot [27].

We have created a synthetic, chemically driven molecular motor that can step autonomously. We have coordinated the catalytic cycles of the feet to create a Brownian ratchet with the characteristics required for directional and processive motion. Work in progress on rigid, extended tracks will allow properties of the motor to be tested directly, including failure mechanisms, fuel- and force-dependent speed and processivity.

\*a.turberfield@physics.ox.ac.uk

Supported by EPSRC, BBSRC, MRC and by the MoD through the Bionanotechnology IRC.

- [1] N. Koumura *et al.*, Nature (London) **401**, 152 (1999).
- [2] R. A. Bissell *et al.*, Nature (London) **369**, 133 (1994).
- [3] D. A. Leigh *et al.*, Nature (London) **424**, 174 (2003).
- [4] S. P. Fletcher *et al.*, Science **310**, 80 (2005).
- [5] B. Yurke *et al.*, Nature (London) **406**, 605 (2000).
- [6] A. J. Turberfield *et al.*, Phys. Rev. Lett. **90**, 118102 (2003).
- [7] J. S. Shin and N. A. Pierce, J. Am. Chem. Soc. **126**, 10 834 (2004).
- [8] W. B. Sherman and N. C. Seeman, Nano Lett. **4**, 1203 (2004).
- [9] Y. Tian and C. D. Mao, J. Am. Chem. Soc. **126**, 11 410 (2004).
- [10] J. Bath and A. J. Turberfield, Nature Nanotech. **2**, 275 (2007).
- [11] P. Yin *et al.*, Angew. Chem., Int. Ed. **43**, 4906 (2004).
- [12] J. Bath, S. J. Green, and A. J. Turberfield, Angew. Chem., Int. Ed. **44**, 4358 (2005).
- [13] Y. Tian *et al.*, Angew. Chem., Int. Ed. **44**, 4355 (2005).
- [14] S. Venkataraman *et al.*, Nature Nanotech. **2**, 490 (2007).
- [15] P. Yin *et al.*, Nature (London) **451**, 318 (2008).
- [16] K. Svoboda *et al.*, Nature (London) **365**, 721 (1993).
- [17] A. D. Mehta *et al.*, Nature (London) **400**, 590 (1999).
- [18] P. Reimann, Phys. Rep. **361**, 57 (2002).
- [19] H. Wang and G. Oster, Appl. Phys. A **75**, 315 (2002).
- [20] B. Yurke and A. P. Mills, Genetic Programming and Evolvable Machines **4**, 111 (2003).
- [21] N. R. Markham and M. Zuker, Nucleic Acids Res. **33**, W577 (2005).
- [22] See EPAPS Document No. E-PRLTAO-101-091848 for experimental details, controls, and supplementary experiments. For more information on EPAPS, see <http://www.aip.org/pubservs/epaps.html>.
- [23] J. S. Bois *et al.*, Nucleic Acids Res. **33**, 4090 (2005).
- [24] S. J. Green, D. Lubrich, and A. J. Turberfield, Biophys. J. **91**, 2966 (2006).
- [25] G. Seelig, B. Yurke, and E. Winfree, J. Am. Chem. Soc. **128**, 12 211 (2006).
- [26] N. J. Carter and R. A. Cross, Nature (London) **435**, 308 (2005).
- [27] C. Veigel *et al.*, Nat. Cell Biol. **4**, 59 (2002).
- [28] R. W. Lymn and E. W. Taylor, Biochemistry **10**, 4617 (1971).